Contrasting Garnet Lherzolite Xenolith Suites from the Letšeng Kimberlite Pipes: Inferences for the Northern Lesotho Geotherm

N. P. Lock and J. B. Dawson

Abstract

The Main and Satellite Pipe kimberlites at Letseng-la-Terae, Lesotho, both contain abundant crustal and mantle xenoliths. In garnet lherzolite xenoliths that are the subject of this paper, textures range from coarse to highly deformed in samples from both pipes, but the most extreme deformation is seen only in Main Pipe samples. Development of reaction coronas around the garnets in all samples indicates retrogression to spinel peridotite facies conditions prior to entrainment in the host kimberlites. Bulk rock compositions of most samples are depleted relative to pristine mantle compositions. Most Main Pipe samples equilibrated at 950–1,000 °C and pressures of 40–45 Kbar, with others extending the temperature range to 820 °C and 1,350 °C. In the temperature range 950–1,000 °C, there is no overlap with Satellite Pipe xenoliths which equilibrated at <800 and >1,305 °C. High-T samples from both pipes lie on the high-T side of the Cretaceous Kalahari geotherm of Rudnick and Nyblade (1999), indicating a perturbed geotherm, similar to that deduced from Thaba Putsoa xenoliths but unlike the non-perturbed geotherm inferred from mantle xenoliths in other Cretaceous Lesotho kimberlites. Hence, xenolith suites from individual kimberlite intrusions each have distinctive thermal characteristics, and there is no consistently perturbed Cretaceous geothermal gradient beneath Lesotho.

Keywords

Garnet lherzolites • PTs of equilibration • Lesotho geothermal gradient

Introduction

Kimberlite pipes and dykes intrude the Karoo (Carboniferous–Triassic) sandstones and basalts in the Maluti Mountains of northern Lesotho, to the east of the major Cretaceous kimberlite province of South Africa (Nixon 1973). Zircon from the Mothae pipe has been dated at 87.1 Ma (Davis 1977), and perovskite from other pipes (Kao, Liqhobong, Lipelaneng, Mothae, Ngopetseu) has yielded ages ranging from 88.8 ± 1.4 to 94.7 ± 1.1 Ma (1 sigma errors—Hoese 2009).

The Main and Satellite kimberlite pipes at Letšeng-la-Terae (29°00′S 28°43′E) (for brevity hereafter referred to as Letšeng) contain abundant crustal and mantle xenoliths and afford the opportunity to compare two peridotite xenolith suites which can reasonably be assumed to have been transported up the same or closely adjacent upper mantle conduit(s). The pipes, which are only ~350 m apart (Fig. 1), crop out at ~3,100 m above sea level, forming the world's highest diamond mine. Features of the bulk diamond production are

N. P. Lock
Coffey Mining, 20 Meteor Drive, Etobicoke, Ontario, M9W 1A4, Canada

J. B. Dawson (✉)
Grant Institute of Geosciences, University of Edinburgh, Edinburgh, EH9 3JW, UK
e-mail: jbdawson@glg.ed.ac.uk

D. G. Pearson et al. (eds.), *Proceedings of 10th International Kimberlite Conference*,
Volume 1, Special Issue of the Journal of the Geological Society of India,
DOI: 10.1007/978-81-322-1170-9_3, © Geological Society of India 2013

the overall low diamond grade but the occasional occurrence of exceptionally large, high-quality (type IIA) diamonds. Harris et al. (1979) and Bowen et al. (2009) report significant differences in diamond morphology and colour, but not of size–frequency distribution, between the diamond populations from the two pipes. An objective of this study is to compare the Letseng xenolith suite with that from Thaba Putsoa, Lesotho, from which a perturbed geothermal gradient has been inferred with implications for major frictional heating at the base of the Kalahari craton (Boyd 1973a).

General Geology

The two pipes (Fig. 1) are separated by basalt wall rock that forms abundant xenoliths in both pipes. In the Lesotho province, kimberlites intruding the Drakensberg basalts have a maximum stratigraphic age of ca 180 Ma (Duncan and Marsh 2006), but the Letseng pipes have not been dated radiometrically. Other xenoliths are of Karoo sediments; gneisses and granulites that have their analogues in the basement of southern Africa; and upper mantle peridotites (*s.l*).

The Main Pipe (surface area 17.2 ha) comprises four petrographically distinct types of kimberlite, the contacts between which are gradational over a few metres (Lock, 1980). The kimberlites are broadly volcanoclastic (terminology of Scott Smith et al. 2008), but with distinctive characteristics, and the pipe is mainly infilled by autolithic kimberlite. This is penetrated by a smaller body of highly garnetiferous kimberlite which is zoned, with increasing abundance and/or size of peridotite xenoliths and garnet megacrysts towards its centre. It is cut by three dykes, which are interpreted as the hypabyssal facies of the garnetiferous kimberlite. Penetrating the garnetiferous kimberlite are two smaller bodies of highly micaceous kimberlite, the younger of which contains fresh olivines. The intrusive relationships between the different kimberlite types suggest a younging towards the centre of the diatreme.

The Satellite Pipe (surface area 5.2 ha) mainly contains kimberlite that is similar to the Main Pipe autolithic kimberlite, though Palmer et al. (2008) recognise five texturally different varieties and, in the south-west part of the pipe, reworked kimberlite that surrounds a major basalt raft. Sedimentary xenoliths are more abundant than in the Main

Fig. 1 The Letšeng kimberlite pipes, showing the distribution of kimberlite types in the Main Pipe at the 55 m level (Lock 1980) and the Satellite Pipe at the 70 m level (Palmer et al. 2008)

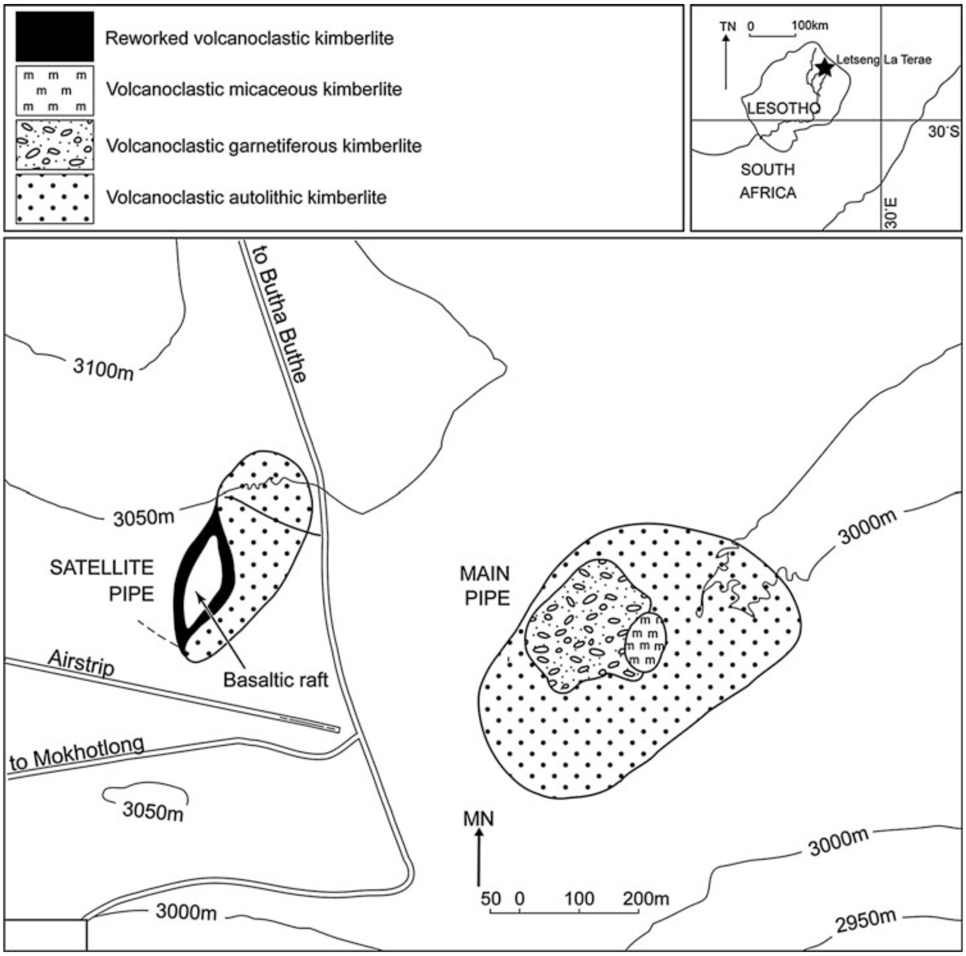

Pipe, whereas peridotite xenoliths are much rarer. An early dyke of micaceous kimberlite is truncated by the pipe. The emplacement of the two pipes is assumed to be pene-contemporaneous, but there are no dates on either intrusion.

Ultramafic Xenoliths

The xenoliths reported here were collected in situ underground from the Main Pipe and from the surface diggings on the Satellite Pipe. However, kimberlite from both pipes is processed at the plant and the xenoliths piled in a common dump; so, when collected from the dump, the source of xenoliths is unclear. In the case of samples studied by Simon et al. (2003), neither texture nor location (?Main or ?Satellite Pipe) is reported so they are here referred to as being from "Pipe not known".

The most common ultramafic xenoliths are garnet or chromite lherzolites and harzburgites, but rarer types are lherzolites containing both garnet and Cr-spinel, garnet dunites, garnet websterites, garnet pyroxenites, Al-spinel lherzolites (some of which also contain garnet) and barren harzburgites (i.e. containing low-Ca–Al enstatites—Hervig et al. 1980). Primary phlogopite is present in a few lherzolites, and secondary phlogopite, generally adjacent to garnet, is present in samples that also show incipient serpentinisation. Most rock types are found in both the Main and Satellite pipes, but garnet lherzolites are approximately three times more abundant in the Main Pipe. Barren harzburgites, in which the orthopyroxenes contain very low amounts of CaO and Al_2O_3 (Hervig et al. 1980), have been recorded only from the Main Pipe.

Petrography

Garnet lherzolites are the focus of this contribution. Measured modes and maximum grain sizes in coarse specimens are as follows: olivine 54–78 modal %, up to 6 mm; enstatite 11–41 %, 8 mm; garnet 3–14 %, 5 mm (including the reaction coronas); and green diopside 0.3–10.3 %, 4 mm. Diopside is often spatially close to garnet. A small number of samples also contain rare chrome-rich spinel or Al-rich spinel (up to 0.3 mm). Grain sizes in deformed rocks are less than in coarse samples.

Due to varying deformation and recrystallisation, the peridotites exhibit a range of textures from coarse texture (not recrystallised), through increasingly recrystallised porphyroclastic and mosaic-structured to laminated and disrupted (LAD) textures (terminology of Harte 1977). In the LAD rocks, garnet and its surrounding reaction coronas are disrupted and strung out into fine-grained chains, interspersed, with laminae of fine-grained olivine and pyroxene neoblasts. Rocks showing recrystallisation are collectively referred to hereafter as "deformed". A range of textures are seen in samples from both pipes (Table 1); however, the Main Pipe suite is dominated by coarse-textured rocks and the most extreme LAD deformation has not been recognised in Satellite Pipe xenoliths.

Whole Rock Chemistry

Due to small xenolith size in some cases, not all samples listed in Table 1 were analysed. Compositions of the analysed samples are given in Table 2, with comparable analyses of other pertinent garnet lherzolites and a reference analysis for primitive mantle. With one high-Fe exception, the Letšeng rocks, whether coarse or deformed, are depleted in TiO_2, Al_2O_3, FeO and CaO relative to the primitive mantle composition. With the exception of the high-Fe sample, the Mg# values (a depletion indicator) of the Letseng lherzolites have a narrow range (91.0–93.2) with a slight tendency for lower values in deformed samples (Fig. 2). Coarse "sterile" (i.e. depleted) and sheared "fertile" (i.e. undepleted) garnet lherzolites from Thaba Putsoa show greater differences. Cr/(Cr + Al) ratios (another indicator of depletion) show a range from 0.149 to 0.367, with an overlap between coarse and deformed samples; however, there is no overall correlation between the two depletion parameters. Also, in the Letseng samples, there is no correlation between degree of depletion and deformation, unlike Thaba Putsoa where high deformation is linked to high "fertility". The Fe-rich sample 3 is also relatively rich in Ti and Ca, and although differing in containing little Na_2O, in both its Mg# and Cr/(Cr + Al) ratio, it strongly resembles Thaba Putsoa fertile lherzolite which has been interpreted as having been metasomatised during the kimberlite event. The bulk compositions of most Letšeng lherzolites are similar to many other Kalahari craton lherzolite suites in Cretaceous kimberlites and also show little compositional difference, in terms of SiO_2, FeO, Al_20_3 and CaO, to off-craton peridotites (Janney et al. 2010). However, they are more refractory than garnet lherzolites in the Proterozoic Premier kimberlite (Table 2), the undepleted composition of which is attributed to sampling before the early Mesozoic major melting/depletion event that produced the Mesozoic Karoo volcanics (Danchin 1979).

Phase Chemistry

Primary Phases

Analyses of the phases in twenty-four garnet lherzolites were carried out by WDS on electron microprobes at the universities of Edinburgh and Cambridge. At Edinburgh,

Table 1 Textures and equilibration conditions of Letšeng garnet lherzolites

Samples	Field Number	Texture	NG85[a]	TA98[b]
Main Pipe—coarse			kb	°C
1	NL001	Coarse	45.3	989
2	NL006	Coarse	40.8	976
3	NL012	Coarse, Fe-rich	41.0	1,017
4	NL103	Coarse	38.8	981
5	NL104	Coarse	39.6	963
6	NL128	Coarse + Cr-spinel	25.8	757
7	NL144	Coarse + phlogopite	40.9	991
8	NL145	Coarse + Cr-spinel	40.1	864
9	NL153	Coarse	36.6	928
10	NL197	Coarse	39.7	973
11	NL492	Coarse	39.9	982
Deformed				
12	NL007	Porphyroclastic	42.0	963
13	NL141	Porphyroclastic	51.6	1,211
14	NL169	Porphyroclastic	49.2	1,190
15	NL426	LAD	42.2	1,029
16	NL427	LAD	40.8	1,015
17	NL441	Porphyroclastic	40.2	1,001
18	NL494	Mosaic porphyroclastic	55.0	1,356
19	NL495	Mosaic porphyroclastic	46.3	1,181
20	PHN2573[c]	"Sheared"	51.1	1,337
21	PHN2575/2[c]	"Sheared"	52.0	1,357
22	PHN2575/3[c]	"Sheared"	50.8	1,347
Satellite Pipe—coarse				
23	BD1870-1	Coarse,	19.3	697
24	BD1870-2[d]	Coarse	30.4	778
25	BD1894	Coarse Fe-rich	18.6	693
Deformed				
26	NL021	Mosaic porphyroclastic	43.5	1,305
27	NL503	Mosaic porphyroclastic	43.5	1,313
28	BD1899	Porphyroclastic	49.2	1337
Pipe not known				
29	LET29[e]	Texture not stated + Cr-spinel	39.0	992
30	LET38[e]	Texture not stated	40.6	987
31	LET64[e]	Texture not stated	41.4	1,020

[a] Pressure by Nickel and Green (1985). [b] Temperature by Taylor (1998)
[c] From Boyd (1973b); [d] From Hervig et al. (1980); [e] From Simon et al. (2003)

where most analyses were performed, the probe was a Cameca SX50, and standards used were the following: for Si and Ca—wollastonite; Ti—rutile; Al—corundum; Fe, Mn—metals; Mg—periclase; Na—jadeite; K—orthoclase; Na and K were analysed early in the routine to avoid migration/volatility effects. Counting times were 30 s on peaks and 15 s on backgrounds. Analyses were performed with a spot beam of ~2 µm at 20 kV and a probe current of 20 nA. Data were reduced using the PAP routine procedure (Pouchou and Pichoir 1991). Our data are supplemented by data on seven additional lherzolites from Boyd (1973b), Hervig et al. (1980) and Simon et al. (2003) (Table 1).

Olivines (Table 3) lie mainly in the compositional range Mg#90–94 with two exceptions, one from each pipe, that

Table 2 Whole-rock analyses of Letseng lherzolites[a] (numbers from Table 1) and other reference samples

		Letseng	Coarse			Letseng	Deformed		
Sample	**1**	**3**	**9**	**10**	**15**	**16**	**17**	**18**	**19**
SiO_2	44.79	45.83	44.93	42.46	47.49	45.31	46.11	44.19	42.60
TiO_2	<0.10	0.11	<0.10	<0.10	0.06	0.07	0.03	0.01	0.09
Al_2O_3	0.89	3.57	0.84	0.61	1.31	0.93	2.44	0.89	0.83
Cr_2O_3	0.40	0.49	0.48	0.23	0.42	0.24	0.88	0.55	0.35
FeO^t	6.35	9.70	6.00	6.99	6.66	7.79	5.96	8.64	8.28
MnO	0.09	0.18	0.91	0.09	0.12	0.14	0.13	0.15	0.11
MgO	46.34	39.12	45.97	48.62	43.04	44.46	43.32	44.28	46.55
NiO	0.30	0.32	0.25	0.29	0.29	0.37	0.28	0.35	0.35
CaO	0.56	0.98	0.38	0.51	0.50	0.50	0.77	0.73	0.72
Na_2O	0.26	0.09	0.22	0.17	0.10	0.21	0.06	0.21	0.11
Mg#	92.8	87.8	93.2	92.5	92.0	91.0	92.8	90.1	90.9
Cr/(Cr + Al)	0.367	0.083	0.280	0.202	0.174	0.149	0.195	0.292	0.221
Sample	**A**	**B**	**C**	**D**					
SiO_2	48.54	44.46	44.31	44.95					
TiO_2	0.00	0.20	0.33	0.158					
Al_2O_3	0.66	2.95	3.40	3.52					
Cr_2O_3	0.26	0.36	0.34	0.385					
FeO^t	5.70	9.59	9.46	7.97					
MnO	0.11	0.15	0.15	0.131					
MgO	44.14	38.19	38.14	39.5					
NiO			0.22	0.252					
CaO	0.50	3.44	2.59	2.79					
Na_2O	0.04	0.33	0.18	0.298					
Mg#	93.2	87.6	88.1	89.6					
Cr/(Cr + Al)	0.207	0.077	0.063	0.067					

A. "Sterile" coarse garnet lherzolite PHN1569, Thaba Putsoa (Boyd and McCallister 1976)
B. "Fertile" sheared garnet lherzolite PHN1611, Thaba Putsoa (Boyd and McCallister 1976)
C. Fertile garnet lherzolite from Proterozoic Premier kimberlite (Danchin 1979)
D. Primitive mantle (Lyubetskaya and Korenaga 2007)
[a] Recalculated on an H_2O^- , CO_2- and K_2O- free basis, and all iron as FeO

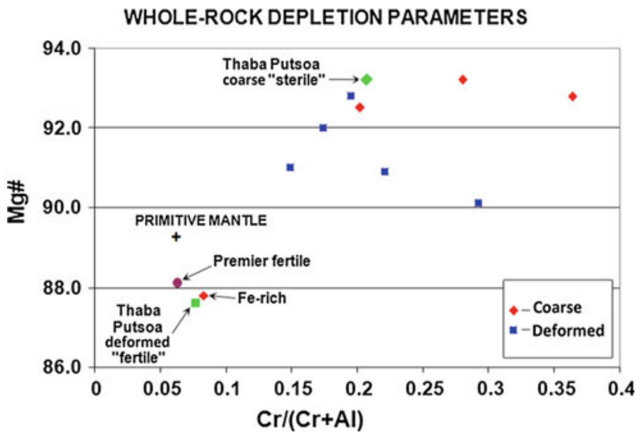

Fig. 2 Bulk rock depletion parameters for Letšeng garnet lherzolites and other mantle compositions. Data from Table 2

are more Fe-rich (Mg# < 90). There are no significant differences in the olivine compositions in coarse and deformed xenoliths, and there is a reasonable correlation between their Mg# and the Mg# of the coexisting pyroxenes and garnet.

Orthopyroxenes (Table 4) show a narrow range of Mg# (91.6–93.7) with the exception of the Fe-rich samples (Mg# 89.8 and 90.7). There is a range in CaO (0.20–1.59 wt%) and, with the exception of the Fe-rich specimens, there is a tendency towards slightly higher Ca and Fe but lower Mg in enstatites from deformed xenoliths in both pipes. All enstatites contain appreciable Al_2O_3 (0.69–1.29 wt %), and those with $Al_2O_3 > 1.2$ wt % are consistently from deformed samples and coexist with subcalcic diopsides ($Ca/(Ca + Mg) < 0.37$).

Table 3 Compositions of olivines in Letšeng garnet lherzolites

Samples	**1**	**2**	**3**	**4**	**5**	**6**	**7**	**8**
SiO_2	41.18	41.09	40.77	41.33	41.14	41.22	42.40	41.36
TiO_2	0.03	0.00	0.03	0.01	0.00	0.00	0.03	0.00
Al_2O_3	0.03	0.05	0.06	0.05	0.10	0.05	0.06	0.06
Cr_2O_3	0.01	0.07	0.00	0.02	0.04	0.00	0.02	0.01
FeOt	7.12	7.72	11.36	7.41	7.70	7.45	7.21	7.32
MnO	0.10	0.10	0.13	0.10	0.12	0.09	0.08	0.10
NiO	0.42	0.39	0.52	0.50	0.40	0.44	0.43	0.43
MgO	51.62	51.24	48.10	51.28	50.79	50.99	51.65	52.02
CaO	0.03	0.04	0.05	0.01	0.04	0.00	0.03	0.03
Na_2O	0.02	0.03	0.04	0.01	0.04	0.01	0.00	0.01
Total	100.56	100.73	101.06	100.72	100.37	100.25	101.91	101.34
Mg#	92.8	92.2	88.3	92.5	92.2	92.4	92.7	92.7
Samples	**9**	**10**	**11**	**12**	**13**	**14**	**15**	**16**
SiO_2	41.42	41.49	41.05	41.17	41.24	41.19	41.09	40.84
TiO_2	0.02	0.02	0.05	0.01	0.09	0.01	0.04	0.04
Al_2O_3	0.02	0.04	0.04	0.03	0.00	0.08	0.06	0.03
Cr_2O_3	0.02	0.02	0.04	0.03	0.05	0.06	0.03	0.02
FeOt	6.99	7.28	7.76	7.96	7.98	7.64	8.02	7.44
MnO	0.08	0.06	0.08	0.11	0.07	0.10	0.10	0.10
NiO	0.38	0.44	0.40	0.38	0.41	0.37	0.44	0.44
MgO	51.88	51.06	50.88	50.55	50.57	51.07	50.85	50.86
CaO	0.02	0.01	0.01	0.01	0.07	0.06	0.04	0.04
Na_2O	0.04	0.03	0.01	0.02	0.04	0.08	0.05	0.03
Total	100.87	100.45	100.32	100.27	100.52	100.66	100.72	99.84
Mg#	93.0	92.6	92.1	91.9	91.8	92.3	91.9	92.4
Samples	**17**	**18**	**19**	**20**	**21**	**22**	**23**	**24**
SiO_2	41.25	40.68	40.35	40.30	40.41	40.00	40.95	40.90
TiO_2	0.03	0.03	0.03	0.03	0.02	0.03	0.00	0.02
Al_2O_3	0.06	0.05	0.05	0.05	0.06	0.09	0.00	0.00
Cr_2O_3	0.01	0.10	0.05	0.04	0.06	0.05	0.00	0.10
FeOt	6.81	8.71	8.81	9.38	9.09	8.84	8.93	8.80
MnO	0.07	0.12	0.10	0.10	0.13	0.12	0.14	0.10
NiO	0.44	0.39	0.40	0.00	0.39	0.38	0.34	0.41
MgO	51.64	50.07	49.97	50.23	50.30	50.66	50.12	50.70
CaO	0.04	0.07	0.05	0.07	0.08	0.09	0.00	0.01
Na_2O	0.03	0.02	0.04	0.04	0.00	0.00	0.00	0.00
Total	100.38	100.24	99.85	100.24	100.54	100.26	100.48	101.04
Mg#	93.1	91.1	91.0	90.5	90.8	91.1	90.9	91.1
Samples	**25**	**26**	**27**	**28**	**29**	**30**	**31**	
SiO_2	41.13	41.19	41.90	41.07	42.0	42.0	41.4	
TiO_2	0.00	0.00	0.00	0.00				
Al_2O_3	0.00	0.00	0.00	0.00	0.01	0.01	0.02	
Cr_2O_3	0.00	0.00	0.00	0.00	0.02	0.02	0.03	

(continued)

Table 3 (continued)

Samples	25	26	27	28	29	30	31
FeOt	10.16	9.05	8.83	9.25	7.25	7.03	7.10
MnO	0.12	0.10	0.10	0.12	0.09	0.08	0.09
NiO	0.34	0.36	0.29	0.37	0.42	0.48	0.44
MgO	49.33	49.91	50.61	49.81	51.4	51.5	51.5
CaO	0.00	0.09	0.11	0.10	0.02	0.03	0.02
Na_2O	0.00	0.00	0.00	0.00			
Total	101.08	100.70	101.84	100.72	101.21	101.15	100.60
Mg#	89.7	91.0	91.1	90.9	92.7	92.9	92.8

Sample numbers from Table 1

Clinopyroxenes (Table 5) range from ureyitic and chrome diopsides to diopsides and subcalcic diopsides (terminology of Stephens and Dawson 1977), with a wide range in Cr_2O_3 (0.75–3.66 wt %). The wide range of Ca/(Ca + Mg) (0.338–0.487) indicates a range of equilibrium temperatures (Davis and Boyd 1966). Subcalcic diopsides (Ca/[Ca + Mg] < 0.40) are present in deformed rocks from both pipes. Intermediate values (0.40–0.46) are common in the clinopyroxenes in Main Pipe samples, but not in those from the Satellite Pipe which have a bimodal grouping of Ca/(Ca + Mg). In the Main Pipe samples, there is no overall correlation between the Ca/(Ca + Mg) ratio and texture, but in coarse samples from both pipes, clinopyroxenes have relatively high Ca/(Ca + Mg) ratios and those from highly deformed samples show relatively low values, with implications for equilibration temperatures.

Garnet compositions (Table 6) show a considerable range in both Mg# (range 78.0–86.5) and Cr content (Cr_2O_3 = 2.77–11.1 wt %); Cr_2O_3 varies directly with CaO and inversely with Al_2O_3. There are no systematic chemical differences between garnets from coarse and deformed rocks in the Main Pipe samples, but those in coarse samples from the Satellite Pipe are more iron-rich than in the deformed rocks and are most similar to the single Fe-rich coarse sample from the Main Pipe. Most, including those co-existing with relatively Fe-rich olivines and pyroxenes, are chrome pyropes (Group 9 of Dawson and Stephens 1975), but one high Ca–Cr garnet in sample 8 is a knorringitic uvarovite pyrope. None is compositionally similar to low-Ca, high-Cr inclusions in diamond.

Spinel A small number of the garnet lherzolites contain magnesian chromite in addition to garnet. Compositionally, in having higher Cr but lower Mg, they are unlike the spinels occurring in both granuloblastic spinel lherzolites and spinel–garnet lherzolites from Letseng (Lock 1980).

Neoblast compositions. Compared with primary grains, both olivine and enstatite neoblasts show no changes in Mg# but consistent, small increases in CaO, for example 0.08 wt % CaO in an olivine neoblast compared with 0.04 wt % in primary olivine. Although this Ca increase might appear small, it is relevant to the whole rock Ca budget due to the modal dominance of olivine in the neoblast population. In the case of deformed clinopyroxenes, the neoblasts contain less CaO, resulting in a slight decrease in the Ca/(Ca + Mg) ratio. Overall lower Ca in the clinopyroxene neoblasts coincides with a concomitant increase in the olivine and enstatite neoblasts. Based on the enstatite solubility in diopside criterion, this can be interpreted as reflecting slightly increased temperatures during recrystallisation.

Conditions of Equilibration of the Letseng Garnet Lherzolites: Inferences for the Lesotho Geotherm

Garnet lherzolites permit calculation of their temperatures and pressures of equilibration, as determined in experimental systems. We have used the two-pyroxene thermometer of Taylor (1998) combined with the Al-in-enstatite in equilibrium with garnet (Nickel and Green 1985) for pressure estimates, as recommended by Nimis and Grütter (2010) in a rigorous review of the various methods of PT calculation. The same methods have also been used to recalculate, for comparison, the data of Boyd (1973a) and Nixon and Boyd (1973), used in their much-discussed model for a perturbed Cretaceous geothermal gradient below northern Lesotho.

The equilibration PTs of the primary assemblages in the Letšeng garnet lherzolites are given in Table 1 and plotted on Fig. 3. Also shown is the Kalahari craton geotherm of Rudnick and Nyblade (1999), which is based on both surface heat-flow and xenolith equilibrium data calculated by the methods of Brey and Köhler (1990); Brey et al. (1990) which, for a given pressure (depth), in most cases give similar temperatures to those obtained by the method used in this paper. Also shown is the graphite–diamond transition of Bundy (1980), preferred to that of Kennedy and Kennedy (1976)

Table 4 Compositions of orthopyroxenes in Letšeng garnet lherzolites

Samples	1	2	3	4	5	6	7	8
SiO_2	57.63	58.19	57.47	57.92	57.64	57.73	58.82	57.25
TiO_2	0.06	0.01	0.13	0.00	0.02	0.01	0.01	0.02
Al_2O_3	0.80	0.72	0.82	0.80	0.77	1.02	0.81	0.76
Cr_2O_3	0.42	0.33	0.22	0.32	0.37	0.35	0.40	0.29
FeOt	4.36	4.67	6.85	4.49	4.78	4.67	4.44	4.39
MnO	0.12	0.12	0.14	0.10	0.10	0.13	0.11	0.12
NiO	0.11	0.13	0.14	0.11	0.15	0.12	0.00	0.16
MgO	35.85	35.77	33.94	35.63	35.62	35.83	36.30	36.70
CaO	0.45	0.48	0.55	0.51	0.49	0.26	0.43	0.39
Na_2O	0.04	0.12	0.18	0.13	0.13	0.08	0.12	0.06
Total	99.84	100.54	100.44	100.01	100.07	100.20	101.44	100.14
Mg#*	93.6	93.2	89.8	93.0	93.2	93.6	93.7	93.8
Ca	1.3	1.0	1.1	0.8	1.0	0.5	0.8	0.7
Mg	92.0	92.3	88.9	92.7	92.1	91.8	92.8	93.0
Fe	6.7	6.7	10.0	6.5	6.9	6.7	6.4	6.3
Samples	**9**	**10**	**11**	**12**	**13**	**14**	**15**	**16**
SiO_2	56.79	58.35	57.55	57.58	57.36	57.60	57.52	57.66
TiO_2	0.05	0.03	0.05	0.13	0.25	0.14	0.09	0.07
Al_2O_3	0.88	0.69	0.79	0.81	0.95	0.96	0.84	0.83
Cr_2O_3	0.50	0.26	0.23	0.46	0.44	0.35	0.36	0.32
FeOt	4.26	4.38	4.67	4.90	4.83	4.59	4.83	4.66
MnO	0.12	0.10	0.09	0.13	0.10	0.12	0.12	0.11
NiO	0.14	0.09	0.10	0.13	0.12	0.13	0.12	0.14
MgO	36.23	35.71	35.60	35.26	34.82	35.14	35.24	35.43
CaO	0.44	0.50	0.48	0.50	0.86	0.93	0.54	0.58
Na_2O	0.19	0.16	0.11	0.16	0.27	0.20	0.16	0.16
Total	99.60	100.27	99.67	100.06	100.00	100.16	99.82	99.96
Mg#	93.8	93.6	93.1	92.8	92.8	93.2	92.9	93.1
Ca	0.9	0.9	0.9	0.9	1.1	1.8	1.0	1.1
Mg	93.0	92.7	92.3	91.9	91.8	91.5	91.9	92.1
Fe	6.1	6.4	6.8	7.2	7.1	6.7	7.1	6.8

Mg# = 100 Mg/(Mg + Fe)

Samples	17	18	19	20	21	22	23	24
SiO_2	57.84	57.25	56.36	56.98	56.90	56.24	57.50	58.30
TiO_2	0.01	0.01	0.20	0.19	0.09	0.16	0.00	0.09
Al_2O_3	0.83	0.94	0.99	1.26	1.16	1.29	1.14	0.87
Cr_2O_3	0.39	0.46	0.40	0.24	0.27	0.26	0.24	0.25
FeOt	4.20	5.22	5.55	5.56	5.18	5.36	5.48	5.38
MnO	0.12	0.15	0.12	0.13	0.15	0.14	0.13	0.11
NiO	0.09	0.17	0.12	0.00	0.00	0.00	0.15	0.10
MgO	35.81	34.32	34.22	34.45	33.75	34.57	35.10	36.00
CaO	0.49	1.59	0.74	1.42	1.34	1.41	0.20	0.26
Na_2O	0.14	0.09	0.26	0.32	0.29	0.35	0.16	0.05

(continued)

Table 4 (continued)

Samples	**17**	**18**	**19**	**20**	**21**	**22**	**23**	**24**
Total	99.92	100.20	98.96	100.55	99.13	99.78	100.10	101.41
Mg#	93.8	92.1	91.7	91.7	92.1	92.0	91.9	92.3
Ca	0.9	3.1	1.5	2.6	3.0	2.6	0.4	0.4
Mg	93.0	89.3	90.3	89.3	89.3	89.6	91.6	91.9
Fe	6.1	7.6	8.2	8.1	7.7	7.8	8.0	7.7
Samples	**25**	**26**	**27**	**28**	**29**	**30**	**31**	
SiO_2	57.79	57.79	58.30	57.59	58.70	58.70	58.30	
TiO_2	0.00	0.00	0.00	0.00	0.01	0.01	0.02	
Al_2O_3	1.33	1.44	1.58	1.28	0.84	0.77	0.77	
Cr_2O_3	0.27	0.34	0.30	0.25	0.36	0.29	0.30	
FeOt	6.28	5.50	5.33	5.52	4.47	4.28	4.27	
MnO	0.12	0.11	0.17	0.16	0.10	0.10	0.10	
NiO	0.12	0.17	0.00	0.14	0.11	0.10	0.12	
MgO	34.50	33.75	34.09	33.69	35.60	35.70	35.50	
CaO	0.22	1.40	1.38	1.46	0.46	0.48	0.48	
Na_2O	0.10	0.36	0.34	0.14	0.15	0.10	0.14	
Total	100.73	100.86	101.49	100.23	100.80	100.53	100.00	
Mg#	90.7	91.6	91.9	91.6	93.4	93.7	93.7	
Ca	0.5	2.7	2.7	2.8	0.9	0.9	0.9	
Mg	90.3	89.2	89.6	89.0	92.6	92.8	92.8	
Fe	9.2	8.1	7.8	8.2	6.5	6.3	6.3	

Sample numbers from Table 1

because a diamond-bearing garnet lherzolite xenolith from the Mothae pipe, 7 km north-west of Letseng (PT conditions 43.0 kb and 1035 °C—Dawson and Smith 1975), plots closer to the diamond stability field of Bundy (1980) although still plotting within the graphite stability field.

From Fig. 3, several facts are apparent:

1. Xenoliths with coarse textures have apparently equilibrated under relatively low PT conditions, though low-temperature estimates (<900 °C) should be treated with caution (Nimis and Grutter 2010).
2. The highest PT conditions are found for deformed xenoliths from both pipes; in this respect, they are similar to high-T, sheared "fertile" xenoliths in the Thaba Putsoa kimberlite (Boyd 1973a). However, a major difference, as noted earlier, is that the Letšeng deformed xenoliths are depleted.
3. The Main Pipe xenoliths (with one exception) have equilibrated along a relatively continuous linear trend, whereas the PT conditions for Satellite Pipe xenoliths are bimodal—one group being low PT, the other at much higher PT.
4. In the Main Pipe xenolith suite, at around 1,000 °C and 40 kb, there is overlap between coarse and deformed xenoliths (including those with the most extreme LAD textures), in this respect being like garnet lherzolite xenoliths from the Kimberley area (Dawson et al. 1975). The most highly deformed xenoliths (i.e. with LAD textures) did not equilibrate at the highest temperatures (see data in Table 1), so there is no overall correlation between the temperature of equilibration and degree of deformation as found at Thaba Putsoa.
5. Many Main Pipe xenoliths, coarse and deformed, derive from an intermediate PT regime apparently not sampled by the Satellite Pipe kimberlite. (The "Pipe not known" samples of Simon et al. (2003) also fall within this PT area).
6. For a given temperature, the Satellite Pipe xenoliths have equilibrated at lower pressures than the Main Pipe xenoliths, thus showing substantial differences in the mantle PT regimes sampled by the two pipes.
7. Compared with the Kalahari craton geotherm, the Main Pipe xenolith linear array is parallel to, but cooler than, the geotherm down to a depth of ~45 kb. The lowest PT xenoliths from the Satellite Pipe plot close to the geotherm, but they are exceptions, and as noted above (a), their temperature estimates should be treated with caution. However, at P > 45 kb, xenoliths from both pipes plot on the high-T side of the geotherm. This indicates a perturbed geotherm as proposed for northern Lesotho by Boyd (1973a).

Table 5 Compositions of clinopyroxenes in Letšeng garnet lherzolites

Samples	**1**	**2**	**3**	**4**	**5**	**6**	**7**	**8**
SiO_2	54.57	54.67	54.99	54.89	54.44	54.44	55.12	53.91
TiO_2	0.10	0.05	0.31	0.00	0.08	0.03	0.03	0.04
Al_2O_3	2.54	1.75	2.75	2.27	2.42	2.05	2.35	1.38
Cr_2O_3	2.65	1.54	1.32	1.80	1.87	1.33	2.88	1.29
FeOt	2.12	2.24	3.61	2.27	2.33	1.66	2.12	1.66
MnO	0.10	0.07	0.10	0.08	0.10	0.08	0.10	0.11
NiO	0.03	0.01	0.08	0.09	0.07	0.04	0.07	0.09
MgO	16.23	17.15	15.85	16.79	16.55	16.62	16.48	17.76
CaO	19.00	20.34	18.49	19.70	19.46	21.98	19.11	22.31
Na_2O	2.38	1.69	2.41	2.03	2.16	1.42	2.37	1.02
Total	99.72	99.51	99.91	99.92	99.48	99.65	100.63	99.57
Mg#	93.2	93.2	88.7	93.0	92.7	94.7	93.3	95.0
Ca	43.9	44.3	42.7	43.9	45.6	47.4	43.7	46.1
Mg	52.2	51.9	50.9	52.1	54.0	49.8	52.5	51.1
Fe	3.9	3.8	6.4	4.0	4.4	2.8	3.8	2.8
Ca/(Ca + Mg)	0.458	0.460	0.456	0.457	0.458	0.487	0.454	0.475
Samples	**9**	**10**	**11**	**12**	13	**14**	**15**	**16**
SiO_2	53.81	55.22	54.36	54.27	54.19	54.72	54.49	54.47
TiO_2	0.07	0.11	0.12	0.31	0.46	0.36	0.29	0.26
Al_2O_3	3.09	2.14	2.12	2.42	2.37	2.15	2.65	2.58
Cr_2O_3	3.66	1.70	1.37	3.13	2.00	1.48	2.08	1.98
FeOt	2.13	2.26	2.18	2.30	2.90	2.71	2.45	2.42
MnO	0.13	0.09	0.11	0.12	0.12	0.09	0.09	0.09
NiO	0.06	0.09	0.01	0.04	0.05	0.05	0.00	0.11
MgO	15.44	16.42	16.98	15.68	17.98	18.34	16.34	16.51
CaO	17.64	19.43	20.13	18.65	17.41	17.98	18.84	18.89
Na_2O	3.13	2.20	1.71	2.55	1.87	1.79	2.18	2.22
Total	99.16	99.66	99.09	99.47	99.35	99.67	99.41	99.53
Mg#	92.8	92.8	93.3	92.4	91.7	92.3	92.2	92.4
Ca	43.3	44.1	44.3	44.1	38.9	39.3	43.3	43.2
Mg	52.7	51.9	52.0	51.6	56.0	55.9	52.3	52.5
Fe	4.0	4.0	3.7	4.3	5.1	4.8	4.4	4.3
Ca/(Ca + Mg)	0.451	0.459	0.460	0.461	0.410	0.413	0.453	0.451
Samples	**17**	**18**	**19**	**20**	**21**	**22**	**23**	**24**
SiO_2	54.46	54.71	54.29	54.43	55.53	55.24	54.24	53.80
TiO_2	0.04	0.03	0.36	0.29	0.15	0.28	0.22	0.26
Al_2O_3	2.42	0.85	2.29	2.46	2.23	2.66	2.62	2.86
Cr_2O_3	2.48	0.75	1.68	0.68	0.74	0.75	1.66	1.56
FeOt	2.11	3.25	3.18	4.04	3.71	3.77	2.11	2.11
MnO	0.11	0.14	0.11	0.14	0.13	0.14	0.00	0.06
NiO	0.06	0.05	0.11	0.00	0.00	0.00	0.00	0.03
MgO	16.39	21.05	18.00	21.16	20.62	20.41	15.68	16.00

(continued)

Table 5 (continued)

Samples	17	18	19	20	21	22	23	24
CaO	18.78	18.25	17.19	15.03	15.20	14.26	20.70	20.60
Na_2O	2.33	0.34	2.06	1.59	1.41	1.77	2.15	2.04
Total	99.18	99.42	99.27	99.82	99.72	99.28	99.38	99.32
Mg#	93.3	92.0	91.0	90.3	90.8	90.6	93.0	93.1
Ca	43.4	36.5	38.4	31.5	32.5	31.3	46.8	46.3
Mg	52.7	58.5	55.9	61.8	61.3	62.3	49.4	50.0
Fe	3.9	5.0	5.7	6.7	6.2	6.4	3.8	3.7
Ca/(Ca + Mg)	0.452	0.384	0.407	0.338	0.346	0.344	0.486	0.480
Samples	**25**	**26**	**27**	**28**	**29**	**30**	**31**	
SiO_2	54.51	55.30	55.82	55.51	55.60	55.20	55.50	
TiO_2	0.23	0.17	0.14	0.00	0.01	0.01	0.11	
Al_2O_3	2.68	1.86	1.79	1.10	2.55	2.00	2.60	
Cr_2O_3	2.11	1.07	1.06	0.53	2.30	1.62	1.71	
FeOt	2.43	3.74	3.51	3.60	2.25	1.90	2.23	
MnO	0.00	0.15	0.00	0.07	0.08	0.09	0.09	
NiO	0.00	0.00	0.00	0.00	0.03	0.04	0.05	
MgO	15.40	20.25	20.66	21.05	16.20	16.90	16.50	
CaO	20.50	15.33	16.16	17.26	18.90	20.40	19.00	
Na_2O	2.34	1.63	1.32	0.75	2.46	1.69	2.28	
Total	100.20	99.50	100.46	99.87	100.38	99.85	100.07	
Mg#	91.9	90.6	91.3	91.2	92.8	94.1	93.0	
Ca	46.6	33.0	33.9	34.9	43.7	44.9	43.5	
Mg	49.1	60.7	60.3	59.3	52.0	51.8	52.5	
Fe	4.3	6.3	5.8	5.8	4.3	3.3	4.0	
Ca/(Ca + Mg)	0.487	0.352	0.360	0.371	0.457	0.464	0.453	

Sample numbers from Table 1

8. The Letšeng PT array ranges from low- to high-PT conditions, in this respect resembling the lherzolites from Thaba Putsoa, but unlike a relatively narrow PT range found in xenolith suites in some other nearby Lesotho kimberlites—Matsoku (Gurney et al. 1975) and Pipe 200 (Carswell et al. 1979)—and from the Kimberley area (Dawson et al. 1975; Boyd and Nixon 1978).
9. Most Main Pipe and all Satellite Pipe samples lie within the graphite stability field.

Conclusions

1. Most Letšeng samples derive from depleted mantle, in this respect being like most lherzolites in other Cretaceous kimberlites. Only a very few samples are more Fe-rich.
2. The garnet lherzolite suites in the two pipes apparently derive from different sections of the upper mantle. This conclusion is in accord with observations that the two pipes have different diamond populations.
3. Some, but not all, deformed xenoliths from both pipes have equilibrated on the high-temperature side of the Kalahari craton geotherm, indicating they were thermally perturbed, but to different extents.
4. Although the thermal perturbation is like that found in deformed rocks from Thaba Putsoa, other xenolith suites from nearby kimberlite pipes do not have this high-temperature overprint. Hence, there is not a consistently perturbed geothermal gradient Lesotho-wide in the upper mantle in the mid-Cretaceous. The reason for these localised thermal differences is debatable, but a possible explanation is differing thermal input into the mantle aureoles surrounding either individual ascending kimberlites or around coarsely crystalline mantle intrusions that have been proposed as the source of the mantle megacryst suites found in most kimberlites (Gurney et al. 1975)

Table 6 Compositions of garnets in Letšeng garnet lherzolites

Samples	**1**	**2**	**3**	**4**	**5**	**6**	**7**	**8**
SiO_2	41.52	41.65	42.03	42.03	41.45	42.04	42.29	41.62
TiO_2	0.07	0.08	0.34	0.00	0.07	0.07	0.01	0.02
Al_2O_3	18.91	19.25	21.18	19.75	19.15	21.68	16.60	15.79
Cr_2O_3	6.71	6.52	2.77	5.90	6.43	3.17	8.77	10.10
FeOt	6.40	6.83	9.78	6.63	6.93	7.61	6.80	6.65
MnO	0.39	0.41	0.41	0.38	0.41	0.47	0.45	0.54
NiO	0.00	0.01	0.04	0.00	0.02	0.01	0.00	0.03
MgO	20.42	19.63	19.40	20.10	19.67	20.17	20.33	16.68
CaO	5.70	6.45	4.73	6.08	6.01	5.43	5.85	8.73
Na_2O	0.04	0.03	0.07	0.01	0.05	0.01	0.02	0.05
Total	100.16	100.86	100.75	100.88	100.19	100.66	101.12	100.21
Ca	14.6	16.6	11.9	15.5	15.4	13.7	14.8	25.4
Mg	72.5	69.8	68.8	71.2	70.6	71.2	71.8	61.0
Fe	12.9	13.6	19.3	13.3	14.0	15.1	13.4	13.6
Samples	**9**	**10**	**11**	**12**	**13**	**14**	**15**	**16**
SiO_2	41.37	41.73	41.98	41.41	42.01	42.25	42.05	41.70
TiO_2	0.07	0.07	0.24	0.32	0.65	0.36	0.10	0.11
Al_2O_3	20.36	19.03	20.88	18.79	19.49	20.39	19.79	19.76
Cr_2O_3	5.83	5.03	3.84	6.39	4.88	4.11	5.47	5.48
FeOt	6.47	6.49	6.98	7.12	6.63	6.14	6.81	6.69
MnO	0.40	0.33	0.36	0.47	0.31	0.30	0.40	0.39
NiO	0.03	0.00	0.02	0.00	0.03	0.00	0.02	0.00
MgO	21.47	20.66	20.85	20.10	21.51	21.98	20.45	20.40
CaO	4.72	5.39	5.14	5.51	4.91	4.85	5.49	5.58
Na_2O	0.06	0.04	0.04	0.08	0.10	0.08	0.07	0.05
Total	100.78	98.77	100.33	100.19	100.52	100.46	100.65	100.16
Ca	12.0	13.8	12.9	14.2	12.2	12.1	14.0	14.3
Mg	75.3	73.4	73.2	71.5	75.0	72.1	72.0	72.4
Fe	12.7	12.8	13.9	14.3	12.8	11.8	14.0	13.3
Samples	**17**	**18**	**19**	**20**	**21**	**22**	**23**	**24**
SiO_2	41.63	41.90	41.28	41.95	41.91	42.37	41.90	41.40
TiO_2	0.09	0.07	0.93	0.58	0.55	0.73	0.14	0.11
Al_2O_3	19.14	18.19	17.92	20.70	20.44	21.02	21.36	21.80
Cr_2O_3	6.47	8.57	6.27	2.34	2.50	2.11	2.94	2.90
FeOt	6.36	5.76	7.15	7.14	6.80	6.45	8.76	8.80
MnO	0.37	0.37	0.34	0.26	0.26	0.25	0.38	0.40
NiO	0.00	0.00	0.03	0.00	0.00	0.00	0.00	0.00
MgO	20.97	17.59	20.46	22.50	22.27	22.14	19.38	19.80
CaO	5.32	6.69	5.64	4.38	4.48	4.16	5.12	4.90
Na_2O	0.03	0.04	0.10	0.04	0.04	0.04	0.00	0.03
Total	100.38	99.18	100.12	99.89	99.25	99.27	99.98	100.14
Ca	13.5	16.8	14.3	10.6	11.0	10.4	13.1	12.4

(continued)

Table 6 (continued)

Samples	17	18	19	20	21	22	23	24
Mg	73.9	70.3	71.7	75.9	76.0	77.0	69.2	70.1
Fe	12.6	12.9	14.0	13.5	13.0	12.6	17.7	17.5

Samples	25	26	27	28	29	30	31
SiO_2	42.10	42.58	43.37	42.80	42.10	42.30	42.10
TiO_2	0.15	0.65	0.35	0.15	0.03	0.02	0.03
Al_2O_3	21.00	19.85	21.05	20.25	19.70	20.40	20.10
Cr_2O_3	3.51	3.59	2.80	3.59	5.85	5.07	4.61
FeOt	9.71	6.91	6.62	7.01	6.63	6.31	6.33
MnO	0.40	0.22	0.22	0.23	0.42	0.37	0.35
NiO	0.00	0.00	0.00	0.00	0.00	0.00	0.00
MgO	18.95	21.75	22.29	21.41	20.30	20.30	20.80
CaO	5.27	4.82	4.70	5.30	5.24	5.49	5.32
Na_2O	0.00	0.00	0.04	0.00	0.02	0.01	0.03
Total	101.09	100.37	101.44	100.74	100.29	100.27	99.67
Ca	13.3	12.0	11.5	13.0	13.5	14.3	13.6
Mg	67.3	74.6	75.8	73.4	73.1	73.0	73.8
Fe	19.4	13.4	12.7	13.6	13.4	12.7	12.6

Sample numbers from Table 1

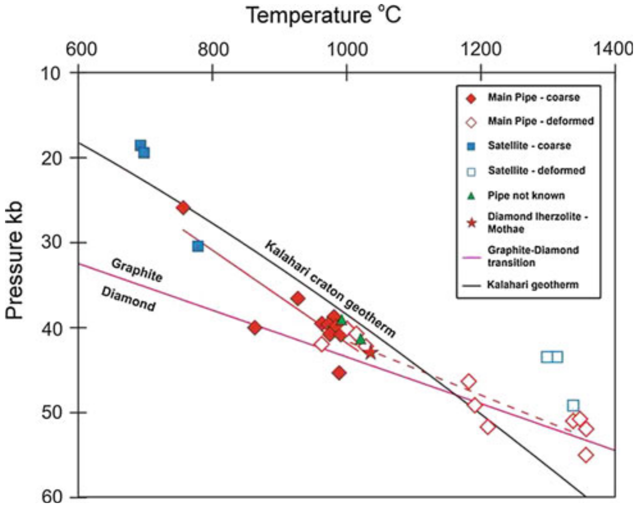

Fig. 3 PT equilibration of Letseng garnet lherzolites (data from Table 1). Other data sources: Kalahari geotherm—Rudnick and Nyblade (1999); graphite–diamond transition—Bundy (1980); Matsoku diamondiferous lherzolite—Dawson and Smith (1975). The solid and broken lines in red are the trends for Main Pipe coarse and deformed xenoliths, respectively

Acknowledgments NPL thanks N.E.R.C for financial support under a Research Scholarship held at the universities of St Andrews and Sheffield, and the Anglo-American Corporation for permission to undertake the research. Whilst NPL was employed with De Beers in Lesotho, Barry Hawthorne and Roger Clement provided encouragement and advice, and Keith Whitelock, the mine manager at that time, laid the foundation for this study. Numerous people helped with the analytical work in St Andrews and Sheffield, and also at Edinburgh, Manchester and Cambridge electron probe laboratories. JBD thanks NERC and the Carnegie Trust for the Universities of Scotland for research funding, and the Organizing Committee of the 10th International Kimberlite Conference for funding that enabled attendance at the Conference. We thank Bill Griffin for drawing our attention to the kimberlite perovskite dates of E. Hoese. Darren Wilkinson drafted the line diagrams. Guest editor H. O'Brien and N.V.C. Rao provided helpful comments which improved the original manuscript.

References

Bowen DC, Ferraris RD, Palmer C, Ward JD (2009) On the unusual characteristics of the diamonds from Letšeng-la-Terae kimberlites, Lesotho. Lithos 112S:767–774

Boyd FR (1973a) A pyroxene geotherm. Geochim Cosmochim Acta 37:2533–2546

Boyd FR (1973b) Appendix of mineral analyses Letšeng-la Terae. In: Nixon PH (ed) Lesotho kimberlites. Lesotho National Development Corporation, Maseru, pp 33–36

Boyd FR, McCallister RH (1976) Densities of fertile and sterile garnet peridotites. Geophys Res Lett 3:509–512

Boyd FR, Nixon PH (1978) Ultramafic nodules from the Kimberley pipes, South Africa. Geochim Cosmochim Acta 42:1367–1382

Brey GP, Köhler T (1990) Geothermobarometry in four-phase lherzolites II. New thermobarometers, and practical assessment of existing thermobarometers. J Pet 31:1353–1378

Brey GP, Köhler T, Nickel KG (1990) Geothermobarometry in four-phase lherzolites I. Experimental results from 10 to 60 kb. J Pet 31:1313–1352

Bundy FP (1980) The P, T phase and reaction diagram for elemental carbon, 1979. J Geophys Res B 85:6930–6936

Carswell DA, Clarke DB, Mitchell RH (1979) The petrology and geochemistry of ultramafic nodules from Pipe 200, northern Lesotho. In: Boyd FR, Meyer HOA (eds) The mantle sample: Inclusions in kimberlites and other volcanics. Proceedings of the second international kimberlite conference, Washington, DC, vol 2. Am Geophys Union, pp 127–144

Danchin RV (1979) Mineral and bulk chemistry of garnet lherzolite and garnet harzburgite xenoliths from the premier mine, South Africa. In: Boyd FR, Meyer HOA (eds) The mantle sample: inclusions in kimberlites and other volcanics. Proceedings of the second international kimberlite conference, Washington, DC, vol 2. Am Geophys Union, pp 104–126

Davis GL (1977) The ages and uranium contents of zircons from kimberlites and associated rocks. Carnegie Inst 76:631–654

Davis BTC, Boyd FR (1966) The join $MgSiO_3$ and $CaMgSi_2O_6$ at 30 Kb and its application to pyroxenes from kimberlite. J Geophys Res 71:3567–3576

Dawson JB, Gurney JJ, Lawless PJ (1975) Palaeogeothermal gradients derived from xenoliths in kimberlite. Nature 257:299–300

Dawson JB, Smith JV (1975) Occurrence of diamond in a mica-garnet lherzolite xenolith from kimberlite. Nature 254:580–581

Dawson JB, Stephens WE (1975) Statistical classification of garnets from kimberlite and associated xenoliths. J Geol 83:589–607

Duncan AR, Marsh JS (2006) The Karoo igneous province. In: Johnson MR, Anhausser CR, Thomas RJ (eds) The geology of South Africa, Johannesburg. pp 501–520

Gurney JJ, Harte B, Cox KG (1975) Mantle xenoliths in the Matsoku kimberlite pipe. Phys Chem Earth 9:507–523

Harris JW, Hawthorne JB, Oosterveld MM (1979) Regional and local variations in the characteristics of diamonds from some southern African kimberlites. In: Boyd FR, Meyer HOA (eds) The mantle sample: Inclusions in kimberlites and other volcanics. Proceedings of the second international kimberlite conference, Washington, DC, vol 1. Am Geophys Union, pp 27–41

Harte B (1977) Rock nomenclature with particular relation to deformation and recrystallisation textures in olivine-bearing xenoliths. J Geol 85:279–288

Hervig RL, Smith JV, Dawson JB (1980) Fertile and barren Al-Cr-spinel harzburgites from the upper mantle: ion and electron probe analyses of trace elements in olivine and orthopyroxene: relation to lherzolites. Earth Planet Sci Lett 50:41–58

Hoese E (2009) The use of perovskite to explore characteristics of kimberlite. Unpubl Honours thesis, Macquarie University, p 52

Janney PE, Shirey SB, Carlson RW, Pearson DG, Bell DR, le Roex AP, Ishikawa A, Nixon PH, Boyd FR (2010) Age, composition and thermal characteristics of South Africa off-craton mantle lithosphere: evidence for a multi-stage history. J Pet 51:1849–1890

Kennedy CS, Kennedy GC (1976) The equilibrium boundary between graphite and diamond. Jour Geophy Res B 81:2467–2470

Lock NP (1980) The geology of the Letšeng kimberlites, Lesotho, Unpublished Ph.D. thesis, University of Sheffield

Lyubetskaya T, Korenaga J (2007) Chemical composition of the Earth's primitive mantle and its variance; 1. Method and results. J Geophys Res B 112:03211

Nickel KG, Green DH (1985) Empirical geothermobarometry for garnet peridotites and implications for the nature of the lithosphere, kimberlites and diamonds. Earth Planet Sci Lett 73:158–170

Nimis P, Grütter H (2010) Internally consistent geothermometers for garnet peridotites and pyroxenites. Contrib Mineral Pet 159:411–427

Nixon PH (1973) (ed) Lesotho kimberlites. Lesotho National Development Corporation, Maseru, p 350

Nixon PH, Boyd FR (1973) Petrogenesis of the granular and sheared ultrabasic nodule suite in kimberlites. In: Nixon PH (ed) Lesotho kimberlites. Lesotho National Development Corporation, Maseru, pp 48–56

Palmer CE, Ward JD, Stiefenhofer J, Whitelock TK (2008) Volcanological processes and their effect on diamond distribution in the Letšeng Satellite Pipe, Lesotho. 9th international kimberlite conference extended abstract no. 9IKC-A-00096

Pochou JL, Pichoir F (1991) Quantitative analysis of homogeneous or stratified microvolumes applying the model "PAP". In: Heinrich KJF, Newbury DE (eds), Electron Probe Quantitation. Plenum Press, New York, pp 31–75

Rudnick RL, Nyblade AA (1999) The thickness and heat production of Archaean lithosphere: constraints from xenolith thermobarometry and surface heat flow. In: Yingwei F, Berika CM, Mysen BO (eds) Mantle petrology: field observations and high pressure experimentation: a tribute to Francis R. (Joe) Boyd. Geochemical Society, Special Publication 6, Houston, pp 3–12

Scott smith BH, Nowicki TE, Russell JK, Webb KJ, Hetman CM, Harder M Mitchell RH (2008) Kimberlites: descriptive geological nomenclature and classification. 9th international kimberlite conference extended abstract no. 9IKC-A-00124

Simon NSC, Irvine GJ, Davies GR, Pearson DG, Carlson RW (2003) The origin of garnet and clinopyroxene in "depleted" Kaapvaal peridotites. Lithos 71:289–322

Stephens WE, Dawson JB (1977) Statistical comparison between pyroxenes from kimberlites and their associated xenoliths. J Geol 85:433–449

Taylor WR (1998) An experimental test of some geothermometer and geobarometer formulations for upper mantle peridotites with application to fertile lherzolite and garnet websterite. Neues Jahrb Mineral. Abhandl 172:381–408John Barry Dawson 1932–2013

John Barry Dawson 1932–2013

Barry Dawson died suddenly at his home in Edinburgh in late January 2013. He will be especially missed by all of his family, colleagues and diverse friends including those of the kimberlite carbonatite and upper mantle community. Barry was known and loved for his wit, charm and conviviality together with his extensive knowledge of kimberlite

geology, poetry, ornithology, and African history. He was a raconteur and a great after-dinner speaker, with a penchant for singing rather rude and amusing songs. Barry was widely regarded as the patriarch of the "kimberlite family". He was well-respected by university faculty, students and industrial geoscientists. Typically, he never held a grudge against persons who held opposing views. Many of us will really miss staying at the "Braid Farm Road Hotel" enjoying the hospitality and G&Ts so generously provided by our host.

Barry was born in Leeds (UK) and attended Leeds University from which he graduated with a B.Sc. in Geology in 1957. His interest in all things African was developed as graduate student with the Research Institute of African Geology. His work there took him to Basutoland (now Lesotho) to study kimberlite intrusions and culminated in his Ph.D (1960). Parts of his thesis appeared in the seminal paper Basutoland Kimberlites (Geol. Soc. America Bull., 73, 1962). This work was the first modern study of kimberlites and was notable in that Barry introduced the term "fluidization" to kimberlite geology; there are still arguments as to the role of this process in diatreme emplacement! Subsequent, to his graduation Barry, and his late wife Christine, embarked again for Africa to join the Tanganyika Geology Survey. It was here he discovered the amazing sodium carbonate volcanism of Oldoinyo Lengai and earned himself a permanent place in petrological history with the publication of his paper in Nature (1962) on these extraordinary rocks. At the time of his death, some 50 years later, Barry was still studying Oldoinyo Lengai and other Tanzanian volcanoes in the Gregory Rift.

In his academic career, Barry was initially employed at the University of St. Andrews (1964–1978), followed by appointment as Sorby Professor of Geology University of Sheffield, and ultimately at the University of Edinburgh 1988–1997. He retired from active teaching in 1997 and continued an active program of research in his two favourite topics; upper mantle-derived xenoliths, and Recent volcanic rocks of northern Tanzania. In recognition of his research he was awarded the Collins medal of the Mineralogical Society of Great Britain in 2012 and the Clough Medal of the Geological Society of Edinburgh (1999). He was a Fellow of the Royal Society of Edinburgh and the German Academy of Scientists.

Barry's involvement with kimberlites continued throughout his life. In particular, he was one of the convenors of the 1st International Kimberlite Conference held in Cape Town (1973) with field excursions led by him and Peter Nixon to Lesotho. This conference resulted in worldwide attention being given to kimberlites and upper mantle-derived xenoliths, and to Barry as "the authority" on all things "kimberlitic". Subsequently, Barry was a convenor of the 2nd Kimberlite Conference held in Santa Fe (1978); an event at which major advances in kimberlite geology were reported; these resulting from studies of the material collected in Lesotho and South Africa. As a consequence of the success of these conferences Barry was instrumental in the formation of the International Kimberlite Conference Advisory Committee and was Chairman of this committee from 1986–1998.

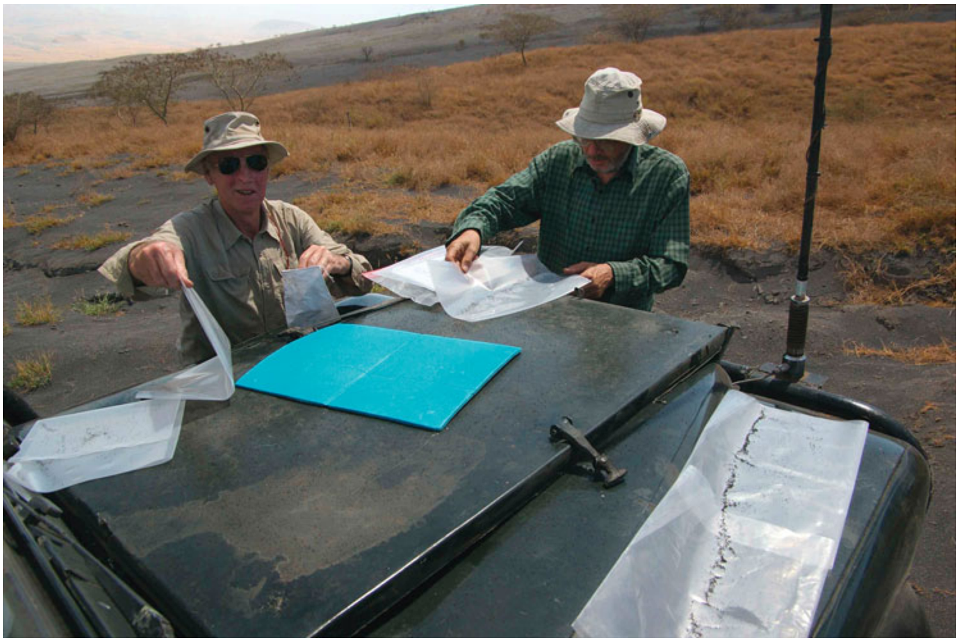

During the last years of his life Barry undertook several expeditions to the Oldoinyo Lengai area, even making the difficult trek to the top of the volcano Kerimasi. As late as December 2012 he was back in Lesotho doing field work. One thing he regretted was that he had not yet climbed all of the Scottish Munros—something he was working on still. His passing is a great loss to us all. To some of us involved in kimberlite and carbonatite research he can never be replaced as he was a mentor and guide throughout our careers. Perhaps Barry was one of the last of the great "gentlemen scientists"?

Roger H. Mitchell
Emeritus Professor of Geology
Lakehead University, Thunder Bay, Ontario
Canada